MBPT and DFT Study of Hydrogen Cyanide Borane(1) Oligomers and Dehydrogenated Analogues†

Adriana Pappová*

Institute of Inorganic Chemistry, Slovak Academy of Sciences, Dúbravská cesta 9, SK-842 36 Bratislava, Slovakia

Ivan Černušák

Chemistry Institute, Faculty of Natural Science, Comenius University, Mlynská dolina, SK-842 15 Bratislava, Slovakia

Miroslav Urban

Department of Physical Chemistry, Faculty of Natural Science, Comenius University, Mlynská dolina, SK-842 15 Bratislava, Slovakia

Joel F. Liebman

Department of Chemistry and Biochemistry, University of Maryland, Baltimore County, 1000 Hilltop Circle, Baltimore, Maryland 21250

Received: November 17, 1999; In Final Form: March 27, 2000

Geometry optimizations and fragmentation energies of the series of hydrogen cyanide borane(1) oligomers (up to hexamers) and their dehydrogenated analogues are presented. Structural parameters are examined at different computational levels: MBPT(2) (second-order many-body perturbation theory), SDQ-MBPT(4) (fourth-order many-body perturbation theory limited to singly-, doubly-, and quadruply excited configurations), and DFT-B3LYP (density functional theory with Becke's three-parameter hybrid functional using the Lee−Yang−Parr correlation functional). These oligomers seem to be suitable input for the models of the polymer chain because of their periodic structure emerging from successive HCNBH or HCNB addition. The stability of the oligomers in terms of initial "cracking" of the weakest bond is fairly high, ranging from 97 to 443 kJ/mol for the HCNBH series and from 329 to 589 kJ/mol for the HCNB series.

Introduction

Sustained experimental[1−5] and theoretical[6−10] interest in the B/C/N materials is motivated by the possibility to adjust their electrical, thermal, and mechanical properties by varying the B/C/N ratio. One of the key roles in understanding these properties is the elucidation of the detailed structure (e.g., graphitic-like networks, nanotubes, or linear arrangements). In this study we investigate theoretically the possibility of the formation of finite linear B/C/N chains from hydrogen cyanide borane(1) as models for these materials.

The idea to model oligomers from hydrogen cyanide borane-(1), e.g., 1-λ^2-2-azonia-1-borata-2-propyne (HCNBH) and 2-azonia-1-λ^1-borata-2-propynyl radical (HCNB), is closely related to our previous calculations.[11−13] We have shown[12] that three forms of $(HCNBH)_2$ exhibit remarkable thermodynamic stability with respect to acyclic monomers (HCNBH or H_2BCN) or cyclic borazirene. The open-chain planar *E*-isomer of $(HCNBH)_2$ consists of two C−N−B segments and can be considered as the *starting point* for the polymer modeling. However, the crucial problem of geometry and stability of longer chains leading to polymers is an open question. The symmetry of the oligomers simplifies the choice of the reference cell in polymer modeling. Careful investigations of the above-mentioned properties in oligomer series must precede any polymer modeling.

We propose two models. The first one, which we denote the $(HCNBH)_n$ model, is generated by repeating the basic HCNBH cell. In the second one we detach hydrogen from boron, thus our basic cell is HCNB. Since we want to work with closed-shell molecules, the simplest way to achieve this is the termination of the chain with a hydrogen atom. However, the molecular formula depends in this case on the number of HCNB units (*n*). If *n* is even, it is convenient to adopt the $H(HCNB)_nH$ model; if *n* is odd, the $(HCNB)_nH$ model. To generalize this notation we will use in the text the formula $\{H\}(HCNB)_nH$.

One can anticipate the impact of electron-donor and electron-acceptor parts in the potential polymer chain to its band structure, and hence to its possible electrical conductivity.[14,15] Suitable substitution of the B and N atoms into the polyacetylene chain combined with the substitution of hydrogen atoms by electron donating groups can tune its band gap and, hence, the conductivity to the values comparable with related polymers (e.g., polyacetylene, polyparaphenylene, or polypyrrole). One can test this assumption on a quasi-infinite chain using the FPC[16] (finite periodic cluster) model. However, the necessary starting point for these calculations is the investigation of oligomers (dimers, trimers, tetramers, etc). The topic of this paper is to derive the possible geometry of the reference cell and to test the stability (or better: thermal viability) of the chain built from it. The reason for finding the best physical model is that in the FPC band gap calculation it is not simple to perform the automatic geometry optimization. Other authors' computational

† Dedicated to Professor Ľudovít Treindl on his 70th birthday.

* Corresponding author. FAX: Int. code +(7)-5941-0444. E-mail: uachpapp@nic.savba.sk.

10.1021/jp9940957 CCC: $19.00
Published on Web 05/27/2000

TABLE 1: Comparison of MBPT(2), SDQ-MBPT(4), and DFT Geometries for HCNBH (Figure 1A)[a]

	CH	CN	NB	BH	HCN	CNB	NBH
MBPT(2)	1.103	1.313	1.255	1.162	107.51	174.39	179.59
SDQ-MBPT(4)	1.121	1.319	1.284	1.170	106.40	173.07	179.99
DFT	1.117	1.298	1.285	1.165	109.05	173.40	178.80

[a] Lengths in Å, angles in degrees.

TABLE 2: Comparison of MBPT(2), SDQ-MBPT(4), and DFT Geometries for H_2CNB (Figure 2A)[a]

	CH		CN	NB	HCN		CNB
MBPT(2)	1.099	1.100	1.272	1.398	120.71	122.23	156.65
SDQ-MBPT(4)	1.100	1.101	1.272	1.407	120.54	122.73	147.17
DFT	1.102	1.102	1.259	1.385	121.68	121.69	179.95

[a] Lengths in Å, angles in degrees.

experience[17,18] provides numerous documentation that small change in the polymer reference cell geometry (especially bond lengths) may cause a considerable change in band gap value.

To better understand this effect we have to consider the effect of the Peierls transition[19] on the bond length alternation and hence, on the electrical conductivity. Polyacetylene is a particularly important example, for, in this case the π-band is half filled, what may eventually result in semiconducting or even metallic properties. According to Peierls, because of the strong intrachain bonding, the π-electrons are delocalized along the polymer chain. When the band is half filled, the tendency toward spontaneous symmetry breaking is particularly strong and it leads to a pairing of successive sites along the chain. This pairing opens the band gap and leads to bond length alternation.[20]

It means that, by the removing of the bond length alternation, it is easy to construct the *nonphysical* polymer model with metallic conduction properties. To avoid this, we have to proceed with the geometry optimization as rigorously as possible.

In the next section, we describe the computational procedure. The Results and Discussion section is divided into three parts. In part I we compare the optimization performance of different methods (MBPT(2), SDQ-MBPT(4), and DFT-B3LYP) and discuss the differences between DFT and MBPT optimized parameters. However, due to computational limitations the geometry optimizations of *all* oligomers up to the hexamer in both $(HCNBH)_n$ and $\{H\}(HCNB)_nH$ models are possible only with the DFT method. Nevertheless, the comparison of MBPT and DFT for smaller systems represents a systematic way to numerically control the quality of geometry parameters. Results of these optimizations are summarized in part II. In our discussion we focus on (1) the central parts of the oligomer chain which are important for the selection of the reference cell, (2) the effect of the terminal part on the geometry of the central part, and (3) the parameters (linearity, periodicity, bond length alternation) that might affect electric properties. Afterward, we suggest the geometry of the $(HCNBH)_n$ and $\{H\}(HCNB)_nH$ reference cell, based on the optimized oligomer geometries. Finally in part III, various fragmentation reactions are proposed to investigate the energetics of the initial "cracking" of the oligomers.

Computational Details

Gradient geometry optimizations have been performed with *Gaussian 94*[21] at SCF, MBPT(2), and DFT-B3LYP levels and with the ACES2 program[22] at the SDQ-MBPT(4) level. For the perturbation calculations the core orbitals were frozen. The DZP basis set[23,24] was used in the majority of calculations. In addition, we used the larger cc-PVTZ basis[25] for selected single-point calculations. The former basis set has been successfully used in numerous correlated studies and has been advocated as a "*minimal correlated basis*" for larger systems.[26,27] The SCF geometries were used as a starting guess for higher level runs. The first part of the calculations includes the comparison of MBPT(2), SDQ-MBPT(4), and DFT-B3LYP methods for smaller systems. The two former methods represent the most popular and affordable correlated levels of geometry optimization that are used for comparison with the DFT approach. SDQ-MBPT(4) can be treated as an approximation to the more rigorous but also more demanding CCSD model (coupled cluster singles and doubles). Due to computational reasons, these exploratory calculations were limited to dimers. In the second step we have performed DFT optimizations of relaxed oligomers. All resulting geometries were subjected to a harmonic frequency check. Full geometry details can be found elsewhere.[28] The stability of the oligomers with respect to initial "cracking" was also investigated. To assist the selection of the potential fragments we have performed additional SCF bond orders calculations[29] (using the program GAMESS[30]) at equilibrium oligomer geometries. The lowest bond orders (and the corresponding Mulliken overlap populations) were taken as indicators of the weakest bonds.

TABLE 3: Comparison of MBPT(2), SDQ-MBPT(4), and DFT Geometries for the Dimer $(HCNBH)_2$[a,b]

	CH	CN	NB	BC	BH	HCN	CNB	NBH	NBC	BCH	BCN
MBPT(2)	1.071	1.181	1.482	1.466	1.190	179.37	179.09	115.01	113.28	121.36	124.69
	1.096	1.372	1.265		1.168	113.96	179.81	179.98			
SDQ-MBPT(4)	1.074	1.166	1.513	1.461	1.193	180.00	180.00	113.79	113.18	121.67	124.91
	1.098	1.383	1.259		1.172	113.42	180.00	180.00			
DFT	1.080	1.179	1.449	1.477	1.191	148.94	176.06	116.23	115.14	120.59	125.46
	1.097	1.353	1.258		1.166	113.95	179.72	179.86			

[a] Lengths in Å, angles in degrees. [b] Two different values for some parameters correspond to the two inequivalent monomer units.

TABLE 4: Comparison of MBPT(2), SDQ-MBPT(4), and DFT Geometries for the Dimer $H(HCNB)_2H$[a,b]

	CH	CN	NB	BC	HCN	CNB	NBC	BCH	BCN
MBPT(2)	1.095	1.280	1.317	1.440	120.71	178.16	177.52	119.03	125.01
	1.095	1.372	1.267		115.97	179.45			
SDQ-MBPT(4)	1.095	1.271	1.321	1.432	120.92	177.94	177.56	119.32	124.99
	1.093	1.379	1.258		115.69	179.35			
DFT	1.095	1.273	1.310	1.434	120.97	179.07	177.38	118.12	126.18
	1.096	1.361	1.256		115.70	178.87			

[a] Lengths in Å, angles in degrees. [b] Two different values for some parameters correspond to the two inequivalent monomer units.

SCHEME 1. DFT-B3LYP fractional charges of the $H^{\delta+}C^{\delta-}N^{\delta+}B^{\delta-}$ segment in $(HCNBH)_2$, (MBPT(2) data in parentheses)

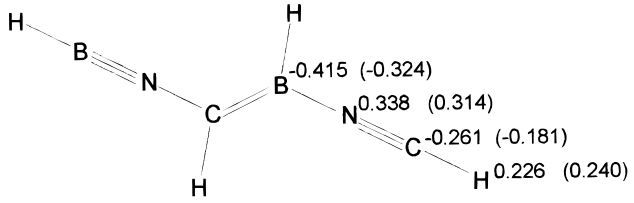

Results and Discussion

I. Comparison of Geometries. The results of geometry optimizations (selected bond lengths and angles) for monomers and dimers at three computational levels are collected in Tables 1−4.

The differences between MBPT(2) and DFT are acceptably small for both the bond lengths and bond angles. We suppose that experimental bond lengths would fall into the interval bracketed by MBPT(2) and DFT results, since MBPT(2) optimization usually overshoots bond lengths.[26,31] The largest deviation occurs for the $(HCNBH)_2$, for which the difference between DFT and SDQ-MBPT(4) single BN bonds is 4.2% (Table 3). Keeping in mind that we are using a minimal correlated basis, this difference is acceptable. As for bond angles, the most striking deviation is for the terminal HCN angle of the same dimer, DFT providing a considerably lower value (148.9°) than MBPT(2) or SDQ-MBPT(4) (180.0°). Apparently the DFT-B3LYP approach slightly exaggerates the charge distribution. In other words, in contrast to MBPT(2), it does not predict the carbon to be sp-hybridized and *tends* to favor sp^2. This tendency can be found also in Mulliken fractional

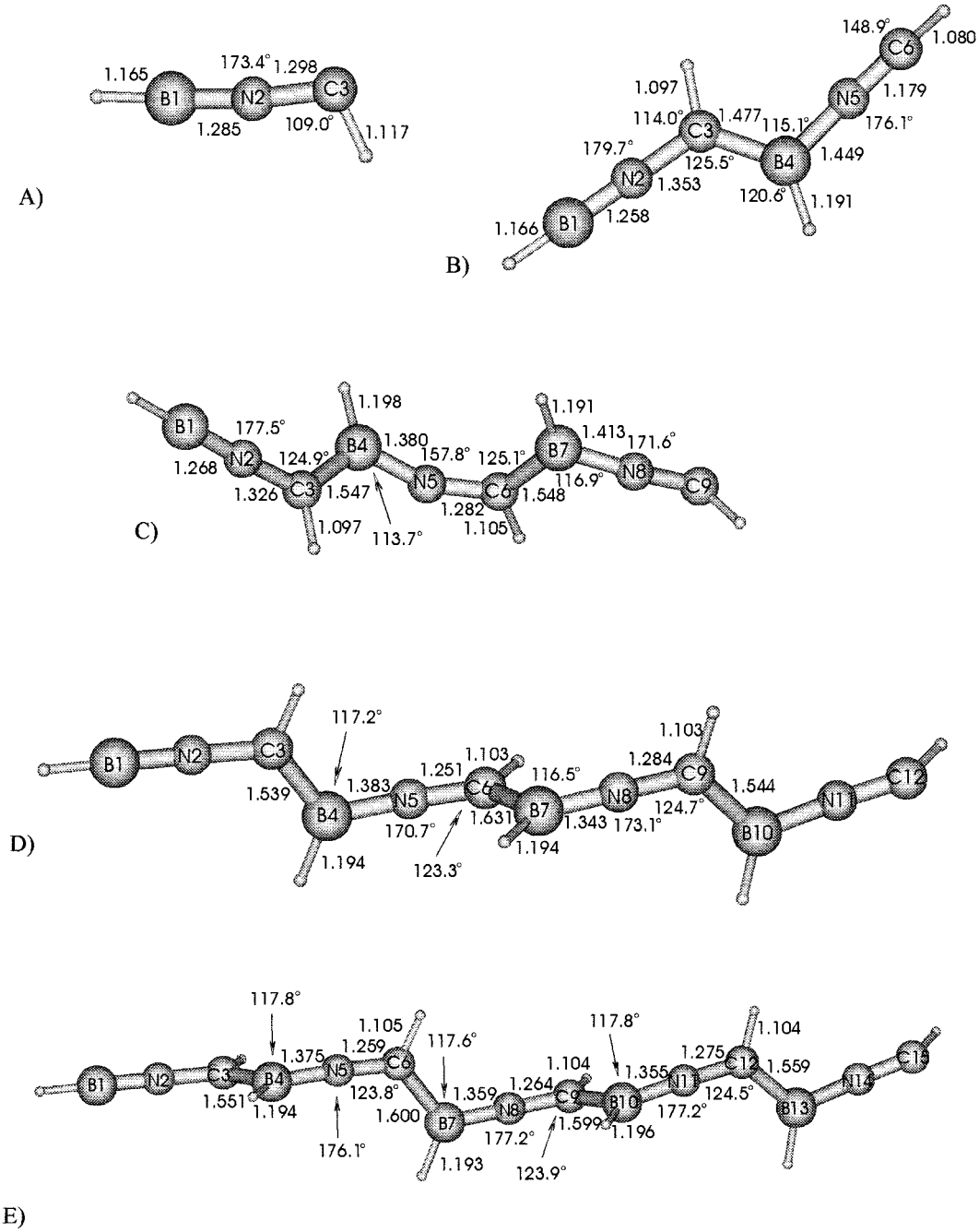

Figure 1. Selected optimized internal coordinates of oligomers in the HCNBH series (bonds lengths in Å, bond angles in degrees): (A) monomer; (B) dimer; (C) trimer; (D) tetramer; (E) pentamer.

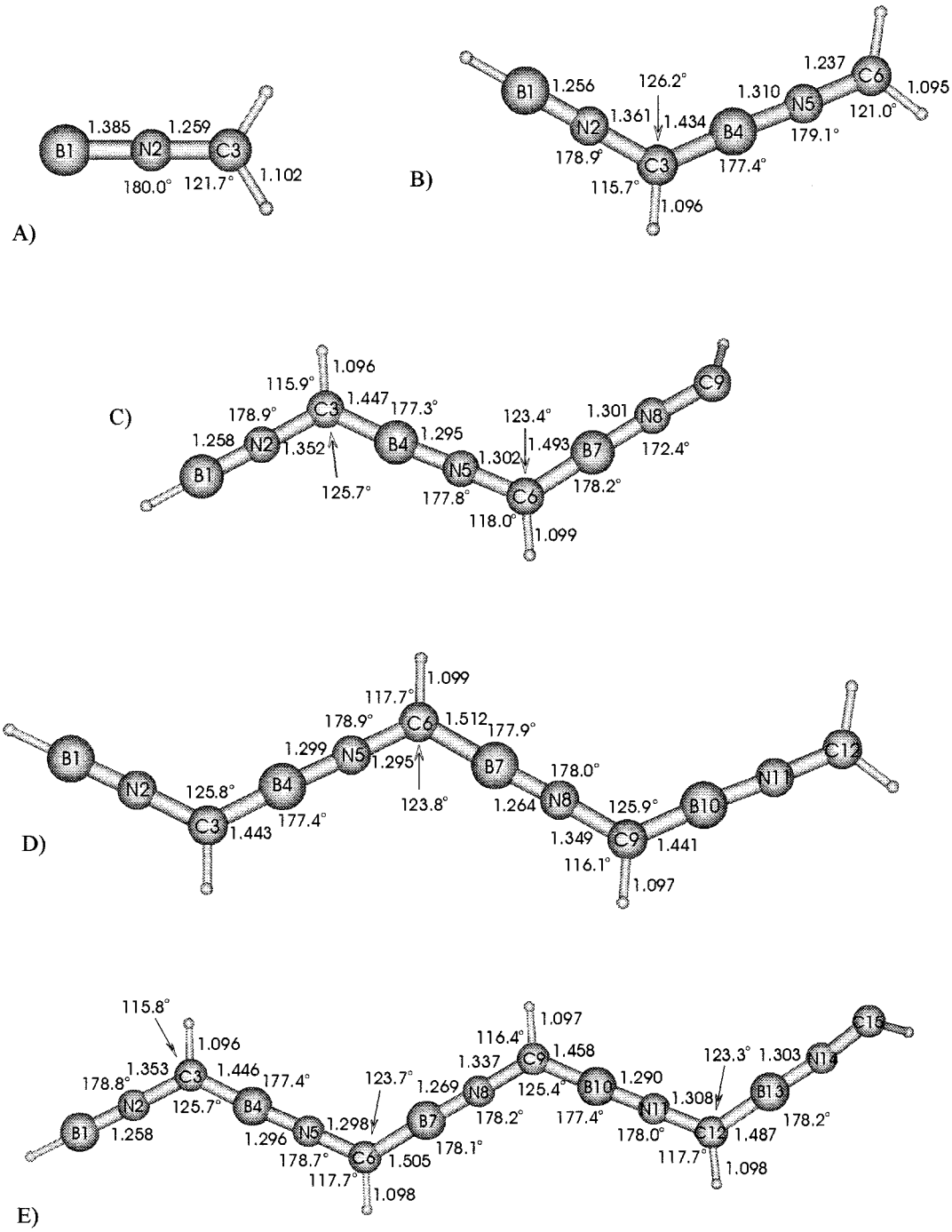

Figure 2. Selected optimized internal coordinates and the fragmentation energies of oligomers in HCNB series. For details see Figure 1.

charges of the $H^{\delta+}C^{\delta-}N^{\delta+}B^{\delta-}$ segment (see Scheme 1, MBPT-(2) values are in parentheses). However, this bending of terminal hydrogen has a relatively small effect on energies. The MBPT-(2) energy difference between DFT and MBPT(2) geometries is −21.8 kJ/mol. Relatedly, the corresponding energy difference calculated at the DFT level is −4.1 kJ/mol, which indicates that the DFT-B3LYP potential energy surface might be rather flat and less sensitive for H-bendings. Conversely, DFT optimization leads to linear CNB in H_2CNB (Table 1), while MBPT(2) and SDQ-MBPT(4) give ∠CNB around 150°. The geometry differences at terminal atoms should have a marginal effect on the central part of the chain with the increasing size of the oligomer (see the next section). Overall, the agreement of all three methods for the central part of the dimers is satisfactory and justifies the use of the DFT-B3LYP model for higher oligomers.

Finally, we have to stress that for geometry optimization of large molecules the DFT-B3LYP approach is the usual alternative, combining efficiency and computational reliability.[31−33] Oliphant and Bartlett have shown that the performance of DFT for geometry optimizations of molecules containing hydrogen and first-row atoms agrees well with experimental results.[34]

II. DFT-B3LYP/DZP Geometry Optimizations. The results of geometry optimizations of oligomers up to hexamers are summarized in Figures 1 and 2. The convergence of important bond lengths observed in central monomeric units is documented in Figures 3 and 4. Before we proceed to the geometry analysis, let us comment on one feature of the HCNBH monomer. Because it is isoelectronic with HCCCH, which is a ground-state triplet,[35,36] we have calculated also singlet−triplet gaps for the monomer and the dimer. The HCNBH itself is a ground-

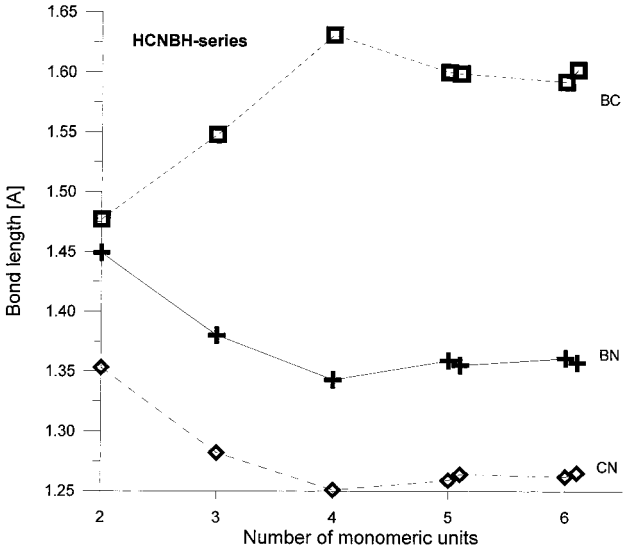

Figure 3. Converging sequence with optimized bond lengths in the HCNBH series with increasing number of monomeric units. Squares refer to BC, diamonds to BN, and crosses to CN bonds, respectively.

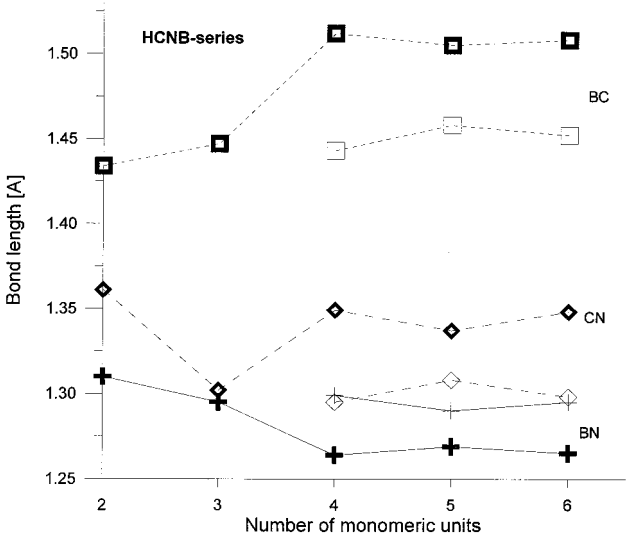

Figure 4. Converging sequence with optimized bond lengths in the HCNB series with increasing number of monomeric units (cf. Figure 3). Bold squares, bold diamonds and bold crosses refer to alternating BC, BN, and CN bonds, respectively.

state singlet, though the triplet lies above the singlet just 14.3 (SDQ-MBPT(4)) or 12.4 kJ/mol (using the more elaborate CCSD(T) model[37]). The respective DFT estimate of the energy gap for the monomer is even smaller (singlet and triplet states are practically indistinguishable). However, the singlet−triplet gap for the dimer calculated from CCSD(T) and DFT energies becomes significantly larger (83.4 and 67.3 kJ/mol, respectively). We do not expect any dramatic changes from ZPV contributions, since the number of degrees of freedom does not change and the geometries in both states are similar.

One can regard the *planar E*-isomer of $(HCNBH)_2$[11,12] as a reference for calculations of higher oligomers. We will refer to this model as the HCNBH series. However, already in the trimer the planarity and the linearity of the BNC sequence are lost (Figure 1C). This effect is due to the presence of the lone pair on the central N atom (the trimer is too short to exhibit delocalization effects as in tetramer or pentamer). Other problems occur when optimizing the geometry of planar $(HCNBH)_4$. The central BC bond in the *planar* tetramer is rather

TABLE 5: DFT-B3LYP/DZP Fragmentation Energies and Enthalpies (kJ/mol) in the HCNBH Series (see also Figure 1)

	DZP		cc-PVTZ
process	ΔE	ΔH_{0K}	ΔE
(1) $(HCNBH)_2 \rightarrow 2HCNBH$	441.1[a]	416.1	443.0
(2) $(HCNBH)_3 \rightarrow HCNBH + (HCNBH)_2$	208.9	193.0	201.5
(3) $(HCNBH)_4 \rightarrow 2(HCNBH)_2$	111.2	100.5	97.2
(4) $(HCNBH)_4 \rightarrow HCNBH + (HCNBH)_3$	343.7	323.6	338.7
(5) $(HCNBH)_5 \rightarrow (HCNBH)_2 + (HCNBH)_3$	222.0	207.6	207.5
(6) $(HCNBH)_5 \rightarrow HCNBH + (HCNBH)_4$	319.7	300.2	311.7
(7) $(HCNBH)_6 \rightarrow 2(HCNBH)_3$	353.3	335.1	
(8) $(HCNBH)_6 \rightarrow (HCNBH)_2+(HCNBH)_4$	218.4	204.5	
(9) $(HCNBH)_6 \rightarrow HCNBH+(HCNBH)_5$	340.1	320.3	

[a] Other levels of theory: SDQ-MBPT(4)/DZP 449.7; CCSD(T)/DZP 449.9 kJ/mol.

weak: indeed, the molecule is unstable with respect to the corresponding fragmentation. Full optimization of the tetramer leads to a stable bent-chain structure with positive (though relatively low) fragmentation energy (see section III). The tetramer possess local translational symmetry of BNC subunits. If one considers the pertinent H atoms as well, the reference cell can be modeled from the dimeric $(HCNBH)_2$ (e.g., −B4-(H)N5C6(H)B7(H)N8C9(H)− in Figure 1D). The neighboring BNCH segments in $(HCNBH)_2$ are almost perpendicular to each other, and each BNCHBHNC sequence is nearly planar. The electron population is higher in the central part of the oligomer for this rotated structure than for the planar one. This fact also explains the lower stability of the planar $(HCNBH)_n$ oligomers, $n > 2$. The fifth representative of this series is the fully relaxed pentamer. Similarly to the tetramer, this structure also represents a bent chain with a well developed dimeric central part in which the two HCNBH subunits resemble the *E*-isomer of $(HCNBH)_2$. The dihedral angle in both central C−B−C−B sequences is approximately 178°, i.e., almost perfect planarity is recovered (see Figure 1E, reading atoms from right to left). In addition, the dihedral angles in the H−B−C−H sequence are also very close to 180°. However, the dihedral angles describing the torsion of hydrogen atoms *within* the HCNBH subunits are still irregular. All structures belonging to the $(HCNBH)_n$ series are depicted in Figure 1. From Figures 1 and 3, the very good convergency of bond lengths along the HCNBH chain for the highest oligomers (the oscillations do not exceed 0.01 Å) is evident. However, there is no alternation of bond lengths in the HCNBH series.

Because our ultimate goal is to find the stable geometry not only for this particular model but also for related models, we decided to modify the original $(HCNBH)_n$ structure by eliminating the boron-bound hydrogen atoms. This led to the {H}-$(HCNB)_nH$ model with sp-hybridized boron and single/double bond alternation (hereafter called the HCNB series). Here, one can expect higher stability due to better electron density saturation on electron-deficient boron atoms. All structures belonging to the HCNB series are depicted in Figure 2.

For the HCNB series, the fully optimized geometry of the central part of all oligomers is close to the optimized planar geometry of the corresponding dimer (Figure 2B). With increasing the chain length, the differences in the shape of the central HCNB subunits are decreasing. Of course, even the geometry of the pentamer can still be affected by boundary effects, but for the hexamer we are able to make a few rigorous observations for the polymer reference cell. First, it is the parallelism of the CBNC subunits (maximum deviation for neighboring parallel CBNC parts is 3.5° for the tetramer, 4.7° for the pentamer, and 3.0° for the hexamer); second is the evident trend in the bond

TABLE 6: DFT-B3LYP Fragmentation Energies (kJ/mol) and Enthalpies in HCNB Series (see also Figure2)

		DZP		cc-PVTZ
	process	ΔE	ΔH_{0K}	ΔE
(10)	$H(HCNB)_2H \rightarrow H_2CNB + HCNBH$	501.5[a]	476.4	499.1
(11)	$H(HCNB)_2H \rightarrow HBN + HCBNCH_2$	599.2	574.0	581.9
(12)	$(HCNB)_3H \rightarrow HCNBH + (HCNB)_2$	502.8	479.4	498.6
(13)	$(HCNB)_3H \rightarrow HCBNCH + HBNCHBN$	345.2	332.4	329.3
(14)	$H(HCNB)_4H \rightarrow HCNBH + H(HCNB)_3$	510.0	476.5	
(15)	$H(HCNB)_4H \rightarrow H(HCNB)_2 + (HCNB)_2H$	461.2	444.8	456.5
(16)	$H(HCNB)_4H \rightarrow HCBNCH_2 + HB(NCHB)_2N$	450.1	428.8	444.9
(17)	$H(HCNB)_4H \rightarrow HBN + (HCBN)_3CH_2$	606.4	581.0	589.3
(18)	$(HCNB)_5H \rightarrow (HCNB)_2CH + HB(NCHB)_2N$	454.1	430.7	450.9
(19)	$(HCNB)_5H \rightarrow (HCNB)_2H + (HCNB)_3$	445.9	427.2	459.5
(20)	$(HCNB)_5H \rightarrow HCNB + (HCNB)_4H$	388.4	367.7	386.6
(21)	$H(HCNB)_6H \rightarrow (HCBN)_3CH_2 + HB(NCHB)_2N$	460.0	438.9	
(22)	$H(HCNB)_6H \rightarrow (HCNB)_4H + H(HCNB)_2$	464.4	446.9	
(23)	$H(HCNB)_6H \rightarrow (HCNB)_5H + H_2CNB$	487.4	464.6	

[a] SDQ-MBPT(4)/DZP 460.3 kJ/mol.

length alternation in the central part of the tetramer and pentamer chains (Figure 2D,E and Figure 4).

Figures 2 and 4 document that (similarly to HCNBH chain) the convergency of bond lengths is very good for the highest oligomers. In addition, Figure 4 reveals clearly the bond alternation in the HCNB model recovered already in tetramer. The bond length alternation indicates that the polymeric analogue of this model is likely to exist in one of two isoenergetic minima resulting from two π-resonance structures.[38] From the electronic structure point of view, we are dealing with the polymer analogous to polyacetylene.

We have found distinct periodicity in both series. According to the geometry trends of the oligomer series we can conclude that it will be necessary to consider the reference cell of two (planar) units in the case of HCNB and of two (perpendicular) units in the HCNBH series, respectively. Since the latter model lacks planarity, one can expect larger band gap. As was mentioned in the previous section, for the HCNB series the deviation from linearity is small, thus it is probably justified to choose the model with linear CBNC segment of the polymer chain bent at the carbon atoms. In the HCNBH series one can expect the linearity in the BNC segment, while the NCBN sector is doubly bent.

III. Polymer Stability Prediction. In this section, we present the fragmentation energies (Tables 5−6) for both series based on DFT-B3LYP/DZP and B3LYP/cc-PVTZ calculations. We focus on the initial "cracking" of the polymer at its potentially weakest sites, not the total thermal degradation. The choice of our fragmentation reactions is guided by Mulliken overlap populations and Mayer's bond orders[29] and, consequently, we inspect the fragmentations of the weakest bonds. The calculated bond orders, as well as the bond lengths, indicate the bond length alternation in all oligomers, the weak (single) BC or CN bonds alternate with the stronger ones.

Let us define the fragmentation energy ΔE corresponding to the process

$$\text{oligomer} \rightarrow \text{fragment(A)} + \text{fragment(B)} \qquad (1)$$

$$\Delta E = E_A + E_B - E_{olig} \qquad (2)$$

All ΔE values are positive, i.e., the oligomer is in each case more stable than its various fragments. One can object that the fragmentation energies could be affected by the basis set superposition error (BSSE). We have estimated the BSSE for three reactions for dimers at the MBPT(2) level using the Boys−Bernardi counterpoise correction method.[39] The geometry of the fragments was not relaxed, since one has to use the same geometry for the subsystems in the Boys−Bernardi procedure. In reaction 1, the BSSE corrected fragmentation energy $\Delta E_{cpc} = 805.9$ and uncorrected $\Delta E = 835.9$; in reaction 7 the $\Delta E_{cpc} = 673.7$ and $\Delta E = 704.4$; and in reaction 8 $\Delta E_{cpc} = 510.6$ and $\Delta E = 545.9$ (all in kJ/mol). Thus, the error associated with the DZP basis set, ϵ_{BBSE}, lies in the range 4−7% of the CPC-corrected fragmentation energies. We expect that this error will be even smaller for larger systems, because the DZP basis is rather compact and BSSE decreases relatively fast with the distance.

Tables 5 and 6 reveal also the trends in energies. For example, one can find rather stable or converging fragmentation energies for certain types of fragments. For instance the elimination of HCNBH from the dimer, trimer, and tetramer (Table 6, reactions 10, 12, and 14) requires ∼500 kJ/mol. In both series, the fragmentation energies and enthalpies are fairly large, though the ΔH_{0K} values are lower due to negative ΔZPV corrections. However, the ZPV corrections should be taken with caution due to the nonrigidity of the oligomers and limited applicability of the harmonic approximation (there is large number of low-frequency modes in higher oligomers). Fragmentation energies in the cc-PVTZ basis are slightly lower for the majority of reactions. Two exceptions are processes 1 and 19. The differences between DZP and cc-PVTZ are bracketed by 2 and 18 kJ/mol, thus the DZP basis performs quite well in this case. In footnotes to Tables 5 and 6 we present also the fragmentation energies for the dimers at higher level of theory (SDQ-MBPT-(4) and CCSD(T)) to estimate the accuracy of the results.

The oligomers in the HCNB series are more stable than those in the HCNBH series. This can be easily explained keeping in mind the electron deficiency of boron. The HCNB model (i.e., without hydrogen) can provide one extra electron for the chain at two-coordinate boron, increasing the electron density along the BNC network and gaining additional stability to the oligomer. In the HCNBH series, the fragmentation can occur most likely at BC bonds (tricoordinate boron, the lowest bond orders), while in the HCNB series both single BC or CN bonds are the possible sites for cleavage. From an energetics point of view, the HCNB model seems to be a slightly better candidate for the polymer. On the other hand, the HCNBH model offers more sites for substitution, opening greater possibility to tune the polymer properties. To generalize a bit, both model polymers should be thermally viable, i.e., one can expect that they will not depolymerize immediately.

Moreover, the stability of the particular chain becomes less crucial if we consider the opportunity of interchain interaction. In this context, the stabilization of two parallel (or antiparallel)

chains via hydrogen bonding and/or B···N donor-acceptor bonding is another topic that deserves future investigation.

Conclusions

In this paper we have investigated the route to the polymer chain on the basis of the exploratory calculations of various oligomers. Extending the chain up to the hexamer, one can generate oligomers of 1-λ^2-2-azonia-1-borata-2-propyne (HCNBH) and 2-azonia-1-λ^1-borata-2-propynyl radical (HCNB) in a systematic way. We have used MBPT and DFT-B3LYP methods and compared their performance for smaller systems. The differences of geometry parameters optimized by these methods were small, thus we have opted for a very efficient DFT-B3LYP method for all higher oligomer optimizations.

The investigation of the HCNBH and HCNB series has provided promising data for the future polymer investigation. For both series, the central parts of higher oligomers (tetramer to hexamer) can serve as the reference cell for the polymer formation. Different types of periodicity were discovered: for the HCNB series the basic motif is planar $(HCNB)_2$, while for the HCNBH series it is staggered $(HCHBN)_2$ with two neighboring HCHBN units perpendicular to each other. Both models exhibit one-dimensional quasi-linear zigzag periodicity and fair stability with respect to the weakest bond "cracking". The existence of the bond length alternation in the HCNB series suggests interesting electrical properties. Our preliminary periodic cluster calculations within the INDO model[40] predict the band gap to be approximately 3.0−4.5 eV for both series, while the MBPT(2) model[16] provides ∼3 eV for the $(HCNB)_n$ and ∼7 eV for the $(HCNBH)_n$. Work is in progress along this line.

Acknowledgment. A.P. thanks the Slovak Literary Fund for partial support and her American colleague for kind hospitality during her stay at UMBC. I.C. is grateful to the Fulbright Commission, Bratislava and USIA/CIES, Washington, DC (Fulbright grant #21037-1996). J.F.L. thanks the Chemical Science and Technology Laboratory of the U.S. National Institute of Standards and Technology for partial support of his studies of chemical energetics. Computer time from the U.S. National Institute of Standards and Technology, Gaithersburg, MD and SAS Computer Center, Bratislava is acknowledged. Part of the calculations was performed using HP9000-780 donated by the A. von Humboldt Foundation. This project was supported by the Slovak Grant Agency, VEGA grants #1/4227/97 and #1/4012/97.

Supporting Information Available: Cartesian coordinates (Xmol format), tables of total energies and details of BSSE calculations for selected reactions. This material is available free of charge via the Internet at http://pubs.acs.org.

References and Notes

(1) Maya, I.; Richards, H. L. *J. Am. Ceram. Soc.* **1991**, *74*, 406.

(2) Saugnac, F.; Teyssandier, F.; Marchand, A. *J. Am. Ceram. Soc.* **1992**, *75*, 161.

(3) Saugnac, F.; Teyssandier, F.; Marchand, A. *J. Chim. Phys.* **1992**, *89*, 1453.

(4) Weng-Sieh, Z.; Cherrey, K.; Chopra, N. G.; Blasé, X.; Miyamoto, Y.; Rubio, A.; Cohen M. L.; Louie, S. G.; Zettl, A.; Gronsky, R. *Phys. Rev. B* **1995**, *51*, 11229.

(5) Kawaguchi, M.; Kawashima, T.; Nakajima, T. *Chem. Mater.* **1996**, *8*, 1197.

(6) Tanaka, K.; Ueda, K.; Koike, T.; Ando, M.; Yamabe, T. *Phys. Rev. B* **1985**, *32*, 4279.

(7) Liu, A. Y.; Wentzovitch, R. M.; Cohen, M. L. *Phys. Rev. B* **1989**, *39*, 1760.

(8) Miyamoto, Y.; Rubio, A.; Cohen, M. L.; Louie, S. G. *Phys. Rev. B* **1994**, *50*, 4976.

(9) Brocks, G. *J. Chem. Phys.* **1995**, *102*, 2522.

(10) Brédas, J.-L. *Adv. Mater.* **1995**, *7*, 263.

(11) Černušák, I.; Urban, M.; Ertl, P.; Bartlett, R. J. *J. Am. Chem. Soc.* **1992**, *114*, 10955.

(12) Černušák, I.; Urban, M.; Stanton, J. F.; Bartlett, R. J. *J. Phys. Chem.* **1994**, *98*, 8653.

(13) Černušák, I.; Liebman, J. F. *Mol. Phys.* **1998**, *94*, 147.

(14) Havinga, E. E.; den Hoeve, W.; Wynberg, H. *Synth. Met.* **1993**, *55*−*57*, 299.

(15) Dantas, S. O.; dos Santos, M. C.; Galvao, D. S. *Chem. Phys. Lett.* **1996**, *256*, 207.

(16) Varga, Š.; Noga, J. Program performing electronic structure calculations of finite periodic clusters (FPC), supports SCF + MBPT(2) calculations of total energies and band gaps of finite clusters with explicit Born-von Karman periodic boundary conditions. Available upon request from uachvarg@savba.sk.

(17) Sun, J.-Q.; Bartlett, R. J. *J. Chem. Phys.* **1996**, *104*, 8553.

(18) Suhai, S. *Int. J. Quantum Chem.* **1983**, *23*, 1239.

(19) Peierls, R. E. *Quantum Theory of Solids*; Oxford University Press: London, 1955; p 108.

(20) Heeger, A. J.; Kivelson, S.; Schrieffer, J. R.; Su, W.-P. *Rev. Mod. Phys.* **1988**, *60*, 781.

(21) Frisch, M. J.; Trucks, G. W.; Schlegel, H. B.; Gill, P. M. W.; Johnson, B. G.; Robb, M. A.; Cheeseman, J. R.; Keith, T.; Petersson, G. A.; Montgomery, J. A.; Raghavachari, K.; Al-Laham, M. A.; Zakrzewski, V. G.; Ortiz, J. V.; Foresman, J. B.; Cioslowski, J.; Stefanov, B. B.; Nanayakkara, A.; Challacombe, M.; Peng, C. Y.; Ayala, P. Y.; Chen, W.; Wong, M. W.; Andres, J. L.; Replogle, E. S.; Gomperts, R.; Martin, R. L.; Fox, D. J.; Binkley, J. S.; Defrees, D. J.; Baker, J.; Stewart, J. P.; Head-Gordon, M.; Gonzalez, C.; Pople, J. A. *Gaussian 94*, revisions D.3 and E.2; Gaussian, Inc.: Pittsburgh, PA, 1995.

(22) Advanced Concepts in Electronic Structure (ACES II): an ab initio program system for performing MBPT/CC calculations, including analytical gradients, methods for excited states, and a number of other unique methods. Stanton, J. F.; Gauss, J.; Watts, J. D.; Lauderdale W. J.; Bartlett, R. J. Quantum Theory Project: University of Florida, Gainesville, FL, 1991. Basis sets were obtained from the Extensible Computational Chemistry Environment Basis Set Database, Version 1.0, as developed and distributed by the Molecular Science Computing Facility, Environmental and Molecular Sciences Laboratory which is part of the Pacific Northwest Laboratory, P.O. Box 999, Richland, WA 99352, and funded by the U.S. Department of Energy. The Pacific Northwest Laboratory is a multiprogram laboratory operated by Battelle Memorial Institue for the U.S. Department of Energy under contract DE-AC06−76RLO 1830. Contact David Feller, Karen Schuchardt, or Don Jones for further information.

(23) Dunning, T. H., Jr. *J. Chem. Phys.* **1970**, *53*, 2823.

(24) Redmon, L. T.; Purvis, G. D.; Bartlett, R. J. *J. Am. Chem. Soc.* **1979**, *101*, 2856.

(25) Dunning, T. H., Jr. *J. Chem. Phys.* **1989**, *90*, 1007.

(26) Urban, M.; Černušák, I.; Kellö, V.; Noga, J. In *Methods in Computational Chemistry*; Wilson, S., Ed.; Plenum Press: New York, 1987; Vol. 1, p 117.

(27) Bartlett, R. J.; Stanton, J. F. In *Reviews in Computational Chemistry*; Lipkowitz, K. B., Boyd, D. B., Eds.; VCH Publishers: New York, 1994; Vol. V, p 65−169.

(28) Cartesian coordinates are at www.qch.uniba.sk/∼cernusak/Oligomers.txt in Xmol format, see also Supporting Information.

(29) Mayer, I. *Chem. Phys. Lett.* **1983**, *97*, 270. Mayer, I. *Chem. Phys. Lett.* **1985**, *117*, 396. Mayer, I. *Theor. Chim. Acta* **1985**, *67*, 315. Mayer, I. *Int. J. Quantum Chem.* **1986**, *29*, 73. Mayer, I. *Int. J. Quantum Chem.* **1986**, *29*, 477.

(30) Schmidt, M. W.; Baldridge, K. K.; Boatz, J. A.; Elbert, S. T.; Gordon, M. S.; Jensen, J. H.; Koseki, S.; Matsunaga, N.; Nguyen, K. A.; Su, S. J.; Windus, T. L.; Dupuis, M.; Montgomery, J. A. *J. Comput. Chem.* **1993**, *14*, 1347.

(31) El-Azahary, A. A.; Suter, H. U. *J. Phys. Chem.* **1996**, *100*, 15056.

(32) Pulay, P. *J. Mol. Struct.* **1995**, *347*, 293.

(33) Zuilhof, H.; Dinnocenzo, J. P.; Chandrasekhar Reddy, A.; Shaik, S. *J. Phys. Chem.* **1996**, *100*, 15774.

(34) Oliphant, N.; Bartlett, R. J. *J. Chem. Phys.* **1994**, *100*, 6550.

(35) Maier, G.; Reisenauser, H. P.; Schwab, W.; Čársky, P.; Špirko, V.; Hess, B. A., Jr.; Schaad, L. J. *J. Chem. Phys.* **1989**, *91*, 4763.

(36) Huang, J. W.; Graham, W. R. M. *J. Chem. Phys.* **1990**, *93*, 1583.

(37) Bartlett, R. J.; Watts, J. D.; Kucharski, S. A.; Noga, J. *Chem. Phys. Lett.* **1990**, *165*, 513. Raghavachari, K.; Trucks, G. W.; Pople, J. A.; Head-Gordon, M. *Chem. Phys. Lett.* **1989**, *157*, 479.

(38) Karabunarliev, S. *J. Phys. Chem.* **1995**, *99*, 14566.

(39) Boys, S. F.; Bernardi, F. *Mol. Phys.* **1970**, *19*, 553.

(40) Noga, J.; Baňacký, P.; Biskupič, S.; Boča, R.; Pelikán, P.; Svrček, M.; Zajac, A. *J. Comput. Chem.* **1999**, *20*, 253.